NJC

ROYAL SOCIETY OF CHEMISTRY

PAPER

View Article Online
View Journal | View Issue

Cite this: *New J. Chem.*, 2022, **46**, 3146

Carboxamide carbonyl-ruthenium(II) complexes: detailed structural and mechanistic studies in the transfer hydrogenation of ketones†

Robert T. Kumah, Paranthaman Vijayan and Stephen O. Ojwach *

Reactions of *N*-(benzo[*d*]thiazol-2-yl)pyrazine-2-carboxamide (**HL1**) and *N*-(1H-benzo[*d*]imidazol-2-yl)-pyrazine-2-carboxamide (**HL2**) ligands with $Ru(PPh_3)_3ClH(CO)$ and $Ru(PPh_3)_3(CO)_2H_2$ precursors afforded the respective organo-carboxamide ruthenium(II) complexes $[Ru^{(II)}(CO)Cl(PPh_3)_2$**L1**$]$ (**Ru1**), $[Ru^{(II)}(CO)H(PPh_3)_2$**L1**$]$ (**Ru2**), $[Ru^{(II)}(CO)Cl(PPh_3)_2$**L2**$]$ (**Ru3**), and $[Ru^{(II)}(CO)H(PPh_3)_2$**L2**$]$ (**Ru4**). The Ru(II) complexes were characterised by NMR, FT-IR spectroscopies, mass spectrometry, micro-analyses, and single X-ray crystallography. The solid-state structures of complexes **Ru1**, **Ru2**, and **Ru4** confirm distorted octahedral geometries around the Ru(II) atoms, containing one bidentate anionic carboxamidate ligand and four auxiliary ligands (PPh_3/CO/H/Cl). All the complexes (**Ru1–Ru4**) displayed moderate catalytic activities in the transfer hydrogenation of a broad spectrum of ketones, giving a maximum turnover number (TON) of 990 within 6 h. The catalytic activities of the Ru(II) complexes were dependent on both the carboxamidate and auxiliary ligands. $^{31}P\{^1H\}$ NMR spectroscopy studies aided in proposing a monohydride pathway for the transfer hydrogenation reaction of ketones.

Received 26th November 2021,
Accepted 17th January 2022

DOI: 10.1039/d1nj05657c

rsc.li/njc

1. Introduction

The development of organometallic based complexes as catalysts in organic reactions is a major research field.[1–3] To date, a considerable number of novel catalysts have been designed in attempts to meet the high demands of valuable industrial and fine chemical products.[4] In the development of a catalyst for homogeneous reactions, an increasing impetus has been placed on ligand designs, which have the ability to modulate the electronic and steric parameters around the metal centre. This ultimately regulates the catalytic activity, stability and chemoselectivity in the organic transformation of interest.[5,6] As a result, many transition metal complexes supported on various ligands bearing well-defined donor atoms have been tailored to achieve the desired catalytic properties. N-Heterocyclic carbenes (NHC),[7] imino-based, amino-phosphines,[8] imino-phosphines,[9] carboxamides,[10,11] thiosemicarbazone,[12] amino-alcohols,[13] phosphoramidites,[14,15] selenium-based ligands[16] among others[17,18] are among the common ligands, which have been utilised in the past few years.

A number of transition metals including first and second-row transition metals complexes[19,20] have been exploited for their possible catalytic properties in the transfer hydrogenation (TH) of ketones with varied outcomes. Notably, Ru(II),[2] Ir(II/III),[21] Os(II), Rh(I/II),[22] Fe(II),[23] Ni(II)[24] and Mn(I)[25,26] represent the broad spectrum of transition metals that have been studied for their prospective catalytic properties. Ruthenium(II) complexes are extensively studied and have proven to be most active catalysts in the transfer hydrogenation of ketones compared to Rh(I/II), Ir(I/III), and Os(II) complexes.[2,27,28] The chemistry and applications of carboxamide ligands have gained appreciable attention.[29] Carboxamide ligands are less expensive and easily synthesized using simple condensation methods compared to the well-established but expensive phosphine based ligand systems.[8–10] Neutral and anionic based carboxamide ligands have also been shown to improve the catalytic activities and stability of the resultant catalysts in the TH reactions.[11,30]

Recently, a number of Ru(II) carboxamide based complexes have been developed and utilised as potential catalysts in some organic transformations including transfer hydrogenation reactions.[31] Notable among them is the Gupta's recently reported Ru(II)–phosphine–carboxamide complexes which demonstrated catalytic activity, TON (Turnover number) up to 99 in TH of ketones.[10] Do and co-workers have also reported half-sandwich Ru(II) complexes bearing the pyridine–carboxamide backbone for TH of ketones and aldehydes and attained turn over number (TON) up to 200.[32]

School of Chemistry and Physics, University of KwaZulu-Natal, Pietermaritzburg Campus, Private Bag X01, Scottsville, Pietermaritzburg 3209, South Africa.
E-mail: ojwach@ukzn.ac.za; Fax: +27 (33) 260 5009; Tel: +27 (33) 260 5239

† Electronic supplementary information (ESI) available: Additional spectroscopic and mass spectral data (NMR, FT-IR and LC-MS spectroscopic data) and graphical representation. CCDC 2086532–2086534. For ESI and crystallographic data in CIF or other electronic format see DOI: 10.1039/d1nj05657c

Heterocyclic such as benzo[*d*]-thiazole and benzimidazole are known to alter the electron density at the metal center, which could have a significant impact on catalytic properties.[33] Benzo-[*d*]-thiazole and benzo-imidazole heterocyclic groups have been integrated with pyridine moieties and their influence on the corresponding metal complexes in terms of catalytic reactions have been studied. For example, Ru(II/III)-pyridyl benzo-imidazole/benzo-thiazole complexes and their propensity in TH of ketones have been reported with moderate catalytic activity (TON up 540) by our group.[34] Therefore, the combination of pyrazine and benzo-[*d*]-imidazole/benzo-[*d*]-thiazole groups with carboxamide functional group could impact greatly on the catalytic properties of the corresponding Ru(II) complexes. For these reasons, the development of Ru(II) complexes of pyrazine-benzo-[*d*]-thiozole/benzo-[*d*]-imidazole carboxamide has ignited our interest to prepare potential catalysts in the TH of ketones. Herein, we report the synthesis of new pyrazine-benzo-[*d*]-thiozole/benzo-[*d*]-imidazole carboxamide Ru(II) complexes with co-ligands; PPh_3, Cl, CO, and hydride (H) and their potential applications as catalysts in the TH reaction of ketones. Detailed structural characterization and mechanistic studies in the transfer hydrogenation of ketones have been carried out and are discussed.

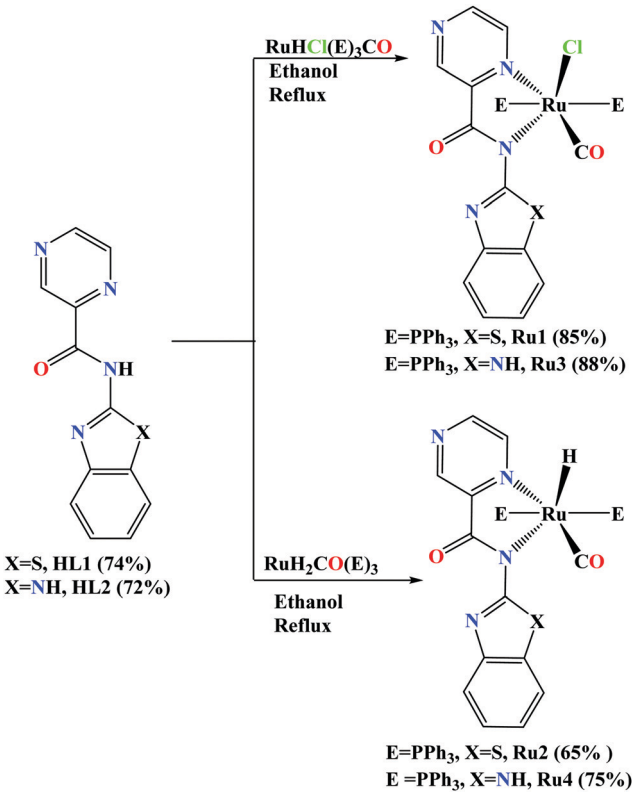

Scheme 1 Synthesis of carboxamide Ru(II) complexes **Ru1–Ru4**.

2. Results and discussion

2.1 Synthesis and characterisation of compounds

The two carboxamide ligands, *N*-(benzo[*d*]thiazol-2-yl)pyrazine-2-carboxamide (**HL1**) and *N*-(1*H*-benzo[*d*]imidazol-2-yl)pyrazine-2-carboxamide (**HL2**) were prepared following literature procedures.[35,36] Detailed synthetic protocol and spectroscopic data of the ligands are provided in the ESI†). The reactions of synthons **HL1** and **HL2** with $Ru(PPh_3)_3ClH(CO)$ and $Ru(PPh_3)_3(CO)_2H_2$ precursors afforded air-stable Ru(II) compounds (**Ru1–Ru4**) in good to high yields (65–88%) as shown in Scheme 1.

The Ru(II) compounds were characterised by ^{1}H NMR, ^{13}C NMR and FT-IR, spectroscopies, mass spectrometry, elemental analyses, and single-crystal X-ray analyses. The signals for the amide proton (N–H) in the ^{1}H NMR spectra of the carboxamide ligands **HL1** and **HL2** were instrumental in the determination of the formation of the Ru(II) complexes (Fig. S1–S6, ESI†). For instance, the ^{1}H NMR spectrum of the carboxamide ligands, **HL1** showed the signal for the N–H_{amide} proton at 12.68 ppm (Fig. S1, ESI†) and upon the formation of **Ru1**, this signal disappeared (Fig. S3, ESI†). This trend was observed in the ^{1}H NMR spectra of the other complexes **Ru2–Ru4** (Fig. S4–S6, ESI†). The absence of the amide proton signal in the ^{1}H NMR spectra of the Ru(II) complexes established the N–H deprotonation upon coordination as depicted in Scheme 1.[36,37] In addition, the new triplet signals at δ_H −13.08 ppm and −13.26 ppm, assigned to the Ru–H protons were observed (Fig. S4 and S6, ESI†) in the ^{1}H NMR spectra of complexes **Ru2** and **Ru4** respectively and assigned to the P–H coupling (t, $^2J_{H-P}$ = 20.3 Hz, $1H_{Ru-H}$).[36] $^{13}C\{^1H\}$ NMR spectroscopy was also relevant in establishing the successful formation of complexes **Ru1–Ru4**. For example, $^{13}C\{^1H\}$ NMR spectrum of complex **Ru1** showed slight shifts in the C=$O_{(amidate)}$ signals (166.8 ppm) in relation to the free ligands **HL1** at 161.3 ppm (Fig. S7–S12, ESI†). While the carbonyl O atom is expected to be non-coordinating (see molecular structures in Fig. 1), these slight shifts could be attributed to electron flow from the **HL1** ligand to the Ru atom, causing a deshielding effect in the carbonyl moiety. Furthermore, the presence of the coordinated pi acceptor carbonyl ligand is expected to favour sigma-donation from the **HL1** ligand to the Ru atom.[36,37] Indeed, this argument is supported by the lower (–Ru–C≡O) signals observed in the ^{13}C NMR spectra, for instance, at 198.1 ppm (typical range for terminal C≡O ligand is 200–210 ppm) for complex **Ru3** (Fig. S11, ESI†).[31] We also made use of $^{31}P\{^1H\}$ NMR spectroscopy to establish the identity of complexes **Ru1–Ru4** (Fig. S13–S16, ESI†). For example, the $^{31}P\{^1H\}$ NMR spectra displayed sharp singlets at δ_P 29.4 ppm (**Ru1**), 48.2 ppm (**Ru2**), 48.2 (**Ru3**) and 23.2 ppm (**Ru4**), consistent with the existence of two magnetically equivalent PPh_3 groups in *trans* configurations.[36]

The successful coordination of the Ru(II) precursors to the carboxamide ligands **HL1–HL2** was further supported by FT-IR spectroscopy. In the FT-IR spectra of complexes **Ru1–Ru4**, the ν(C=O) absorption band shifted to lower frequencies between 1621–1629 cm^{-1} in the complexes with respect to the free ligands of 1691 cm^{-1} (**HL1**) and 1684 cm^{-1} (**HL2**). This observation could be attributed to resonance enhancement of the coordinated ligands leading to weakening of the carbonyl bond.[38] In addition, the terminal carbonyl (–Ru–C≡O) signals were recorded in the region of 1935–1947 cm^{-1}. These values

are relatively lower compared to the values expected for terminal C≡O ligands (2000–2100 cm^{-1}). The presence of sigma-donor spectator **HLI** and **HL2** ligands may account for this observation.[36] As reported in the ^{1}H NMR spectral data, the signals corresponding to N–$H_{(amidate)}$ at 3251–3315 cm^{-1} in the free ligand disappeared upon metalation (Fig. S17–S22, ESI†).[39,40] LC-MS spectra of the compounds gave the signals corresponding to their respective fragments; for example, m/z = 909.12 $[M–Cl]^+$ (**Ru1**), 909.12 $[M–H]^+$ (**Ru2**), 892.15 $[M–Cl]^+$ (**Ru3**), and 892.15 $[M–H]^+$ (**Ru4**) (Fig. S23–S28, ESI†). Furthermore, the experimental and calculated isotopic mass distribution were in good agreement as given in Fig. S23–S28 (ESI†). Notably, the experimental elemental analysis data compared favourably with the proposed empirical formulae, thus establishing both the empirical formulae and purity of the complexes.

2.2 Solid-state structure of complexes Ru1, Ru2, and Ru4

Molecular structures of the complexes **Ru1**, **Ru2** and **Ru4** were confirmed by single-crystal X-ray crystallography analyses. The perspective views of their solid-state structures are shown in Fig. 1, while the refinement data and selected bond parameters are presented in Tables S1 and S2 (ESI†) respectively. The solid-state structures of complexes **Ru1**, **Ru2** and **Ru4** have a distorted octahedral geometry around the Ru(II) centre, with the carboxamide ligand oriented nearly in the plane as defined by the Ru(II) centre and the two *trans* PPh_3 co-ligands. The fifth and sixth coordination sites are occupied by either CO, Cl or H co-ligands to complete the octahedral geometry. The solid-state structures of complexes **Ru1**, **Ru2**, and **Ru4** reveal that the Ru(II) atoms coordinate to the carboxamide ligands **HL1** and **HL2** *via* the pyrazine and amidate N-atoms to form five-membered metallocycles; N(1)–C(4)–C(5)–N(2)–Ru(1). The average bond distance of Ru(1)–$N(2)_{amidate}$ (2.114(3) Å), Ru–$N_{pyrazine}$ (2.118(12) Å), Ru–P (2.400(11) Å), Ru–Cl (2.390(10) Å) and Ru–CO (2.421(11) Å) in complexes **Ru1**, **Ru2** and **Ru4** respectively are within the average bond lengths of Ru–$N_{amidate}$ (2.115(10) Å), Ru–$N_{pyrazine}$ (2.122(12) Å, Ru–P (2.383(12) Å), Ru–Cl (2.410(10) Å) and Ru–CO (1.819(15) Å) found in 8 similar Ru(II) structures deposited in the CCDC.[41,42] The bite angles of the three-membered chelating ring N(1)–Ru–N(2): 77.84(13)° (**Ru1**), 76.13(5)° (**Ru2**), and 76.63(8)° (**Ru4**) are within the mean bite angles of 76.48(5)° found in 8 similar Ru(II) complexes deposited in CCDC file.[41] The average P(1)–Ru–P(2) bond angles in complexes **Ru1**, **Ru2** and **Ru4** of 169.96(8)° deviate significantly from the ideal linearity, 180°. The slight deviation from the linearity of $N(1)_{pyrz}$–Ru–$C(13)_{carbonyl}$ 176.46(14)° in the complexes **Ru1**, **Ru2** and **Ru4** was also observed and could originate from steric restrictions imposed by the bulkier PPh_3 groups on the five-membered ruthenacycle. In addition, the average $N(1)_{pyrz}$–Ru–Cl(1) bond angles of 89.68(8)° and N(1) $_{pyrz}$–Ru–H, 92.80(2)° in compounds **Ru2** and **Ru4** show slight deviations from the ideal bond angle of 90°.

2.3 Application of complexes Ru1–Ru4 in the transfer hydrogenation of ketones

Preliminary investigations of the potential of the Ru(II) organocarboxamide complexes (**Ru1–Ru4**) to catalyse the (TH) of ketones was carried using complex **Ru3**, acetophenone as the model substrate, isopropyl alcohol as a source of hydrogen and KOH as a base. The conversion of the substrates to their respective products was followed and determined using ^{1}H NMR spectroscopy (Fig. S28–S44, ESI†). Percentage conversions of 53% was realised within 6 h at catalyst loadings of 0.10 mol% (Table 1, entry 1). In general, comparable percentage yields of crude products and conversions were realised, thus percentage yields have been adopted in the entire discussion.

2.3.1 Optimization of catalyst loading using complex Ru3.

Having established that the complexes do catalyse the TH of ketones, we then focused on the optimization of the reaction conditions. First to be examined was the catalyst loading, which was investigated by varying catalyst **Ru3** loadings from 0.10 to 1.00 mol% (Table 1). It was noted that an increase in catalyst concentration from 0.100 mol% to 1.00 mol% led to an increase in percentage conversion from 53% to 98% (Table 1, entries 1 and 5). However, an increase in catalyst loading was followed by a decrease in TONs (Table 1 and Fig. S46, ESI†). For instance, TONs of 530 and 97 (maximum conversion after 6 h) were observed at catalyst loadings of 0.10 mol% and 1.00 mol% respectively (Table 1, entries 1 and 5). From this trend, it is clear

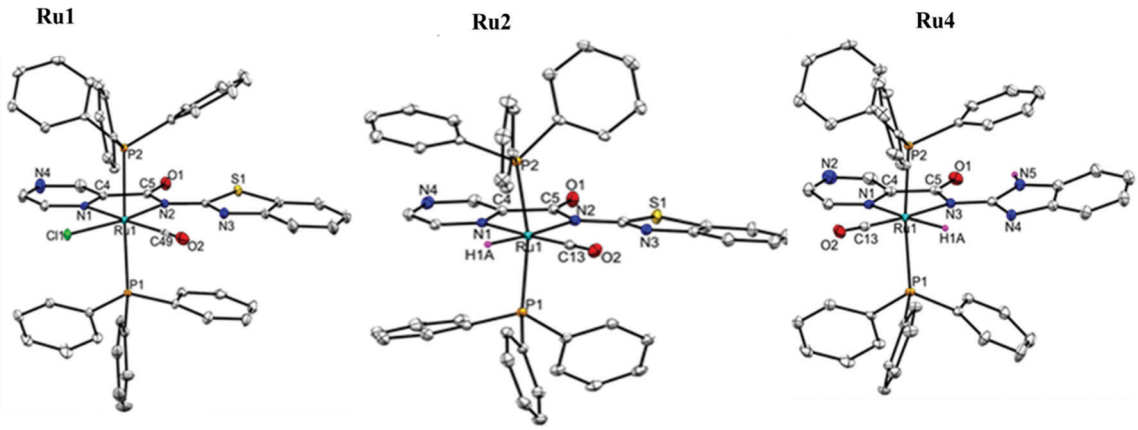

Fig. 1 The ORTEP view of complexes **Ru1**, **Ru2** and **Ru4** with thermal ellipsoids at a 50% probability level. (Hydrogen atoms are omitted for clarity.)

Table 1 Optimisation of catalyst loading for effective TH of acetophenone using complex **Ru3** as pre-catalyst[a]

Entry	Catalyst loading/mol%	Conversion[b] (%)	Yield[b] (%)	TON[c]	TOF[d]/h^{-1}
1	0.10	53	52	530	88
2	0.15	59	58	393	65
3	0.25	68	66	272	34
4	0.50	79	79	158	20
5	1.00	98	97	97	16

[a] Reaction conditions: acetophenone, 1.00 mmol; KOH (0.100 mmol in 5 mL of ^{i}PrOH), anisole (1.00 mmol) was used as internal standard 82 °C time, 6 h. [b] Determined by ^{1}H NMR spectroscopy (experiment repeated in triplicate to ensure reproducibility). [c] TON = moles of acetophenone converted per moles of **Ru3**). [d] TOF = (moles of acetophenone converted per moles of **Ru3** per hour).

while the percentage conversions increased with catalyst loadings, this was not commensurate with the amount of catalyst added, possibly due to catalyst aggregation and is in good agreement with the previous observation made by Ojwach and co-workers where a further increase in catalyst loading did not result in a significant increase in conversion.[34]

2.3.2 Investigation of the effect of nature and concentration of base on the TH reactions. To fully understand the effect of the base in the TH of ketones, we carried out a number of control experiments. First, an experiment using KOH base alone without the ruthenium complex was conducted and afforded percentage conversions of 5% (6 h) and 16% within 36 h (Table 2, entries 1 and 2) and are consistent with the findings reported by Polshettiwar *et al.*[43,44] This is much lower compared to the percentage conversions of 86% (6 h) reported using the **Ru3**/KOH system (Table 2, entry 9), thus confirming that the catalytic activities observed are due to the Ru(II) carboxamide complexes. In another control experiment, we used complexes **Ru3** and **Ru4** without adding any base. More significantly, percentage conversions of 39% in 6 h (Fig. S47, ESI†) and 93% (18 h) were obtained for the hydride complex **Ru4** and 93% (36 h) for the non-hydride complex **Ru3** under base free conditions (Table 2, entries 3–5). The higher catalytic activities observed for the hydride complex **Ru4** in comparison to the non-hydride complex **Ru3** under base free conditions, further reinforced the significance of the Ru–H moiety in the formation of the active intermediates.[45]

To establish the effects of the base loading on the rate of TH of acetophenone reaction, the concentration of KOH was varied from 0.025 mmol (2.5 mo1%) to 1.00 mmol (100 mol%) at constant catalyst loading (0.10 mol%) using complex **Ru3** (Table 2, entries 6–10). From Table 2, it is evident that higher rates of the reactions were achieved at higher base loadings. For instance, TOF of up to 40 h^{-1} and 120 h^{-1} were obtained at base loadings of 2.5 mol% (0.025 mmol) and 7.5 mol% (0.075 mmol) as listed in Table 2, entries 6 *vs.* 8. The nature of the base in controlling the catalytic activity of the complexes in the TH of acetophenone was also investigated using K_2CO_3, NaOH and K^{t}BuO (Table 2, entries 11–13). Expectedly, K^{t}BuO gave the highest catalytic activity, and the observed order of K^{t}BuO > KOH > NaOH > K_2CO_3 tally with the relative strengths of the bases.[34]

Table 2 Optimisation of base loading for effective TH of acetophenone using complexes **Ru3** and **Ru4**[a]

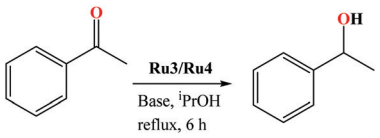

Entry	Base	Catalyst	Base loading/mol%	Time/h	Conversion[b]/%	TOF[c]/h^{-1}
1	KOH	—	10.0	6	5	—
2[d]	KOH	—	10.0	36	16[d]	—
3[e]	—	**Ru4**	—	6	39	65
4[f]	—	**Ru4**	—	18	99	28
5[g]	—	**Ru3**	—	36	93	51
6	KOH	**Ru3**	2.5	6	24	40
7	KOH	**Ru3**	5.0	6	61	102
8	KOH	**Ru3**	7.5	6	72	120
9	KOH	**Ru3**	10.0	6	86	143
10	KOH	**Ru3**	100.0	6	97	164
11	K^{t}BuO	**Ru3**	10.0	6	91	152
12	K_2CO_3	**Ru3**	10.0	6	30	50
13	NaOH	**Ru3**	10.0	6	42	70

[a] Reaction condition: acetophenone, 1.00 mmol; [**Ru3**], 0.100 mol%; ^{i}PrOH, 5 mL; time, 6 h. [b] Determined by NMR spectroscopy internal standard (methoxybenzene). [c] TOF (turnover frequency) = moles of substrate converted per moles of catalyst per hour. [d] Reaction without a catalyst, reaction time, 24 h. [e] Base-free reaction using **Ru4**, time, 6. [f] Base-free reaction using **Ru4**, time, 18 h. [g] Base-free reaction using **Ru3**, reaction = 36 h (all experiments were conducted in triplicate to ensure reproducibility).

2.3.3 Investigation of the role of complex structure on the TH of acetophenone. The optimized reaction conditions of catalyst (0.10 mol%) and K^{t}BuO (10.0 mol%) loadings at 82 °C were then employed to investigate the role of the complex structure (**Ru1–Ru4**) in the TH of acetophenone (Table 3). From Table 3, Fig. 2 and Fig. S49 (ESI†), it was evident that the ligand motif played a crucial role in regulating the catalytic activities of the complexes. For instance, complex **Ru3**, containing the *N*-(1*H*-benzo[*d*]imidazol-2-yl)pyrazine-2-carboxamide (**HL2**) ligand, displayed a higher TOF of 152 h^{-1} (k_{obs} of 2.02 × 10^{-1} h^{-1}) than complex **Ru1**, anchored on the *N*-(benzo[*d*]thiazol-2-yl)pyrazine-2-carboxamide ligand **HL1** (TOF of 118 h^{-1} and k_{obs} of 1.32 × 10^{-1} h^{-1}). This can be rationalised from the basicity of ligands **HL1** and **HL2**, where **HL2** is less basic. This increases the electrophilicity of the Ru metal atom in complex **Ru3** and is in good agreement with its higher catalytic activity.[34,46–48] In terms of the role of the auxiliary ligands, the Ru–H complexes, **Ru2** and **Ru4** showed higher catalytic activities compared to the Ru–Cl analogues, **Ru1 and Ru3**. This can be rationalised from a mechanistic perspective, where the Ru–H intermediate is considered the most active part of the catalytic cycle and required less or no further activation in its reactions compared to the pre-catalysts **Ru1** and **Ru3**.[10,36] This trend is in tandem with the previous report by Gupta and co-workers where the Ru-hydride containing complexes demonstrated higher catalytic activity compared with the non-hydride Ru complexes.[10]

It is also instructive to note that the Ru–H complexes **Ru2** and **Ru4** required lower base loadings of 2.5 mol% in comparison to the 10 mol% used for the non-hydride complexes **Ru1**,

Table 3 Transfer hydrogenation of acetophenone data of complexes **Ru1–Ru4**[a]

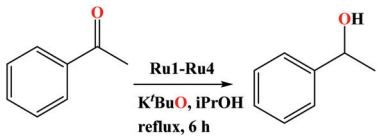

Entry	Complex	Conversion[b] [%]	TOF[c]/h^{-1} × 10^2	k_{ob} × 10^{-1}
1	**Ru1**	71	1.18	1.32(±0.01)
2[d]	**Ru2**	94	1.46	2.02(±0.02)
3	**Ru3**	91	1.52	1.40(±0.04)
4[d]	**Ru4**	99	1.52	2.08(±0.01)

[a] Condition: acetophenone, 1.00 mmol; K^{t}BuO; [Ru], 0.100 mol%; ^{i}PrOH, 5 ml; 82 °C, time, 6 h. [b] Determined by NMR spectroscopy (mean values of two independent runs) by employing methoxybenzene was used as internal standard. [c] TOF (turn over frequency) = moles of acetophenone converted per moles of **Ru3** per hour). [d] Base loading of 2.5 mol% (all experiments were carried out in triplicate to ensure reproducibility).

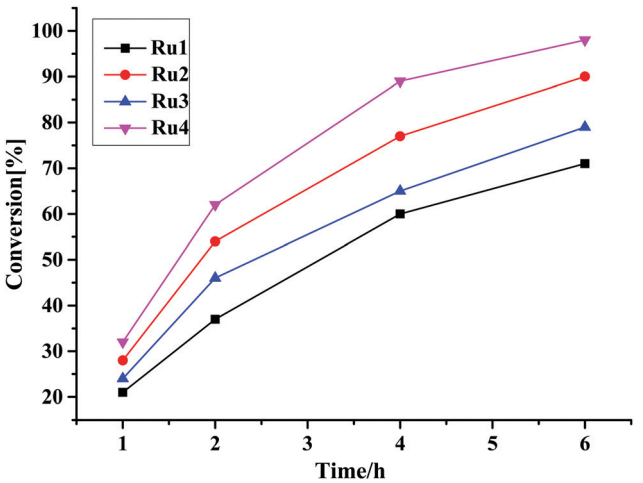

Fig. 2 Plots of percentage conversion *vs.* time showing the effects of catalyst structure on the catalytic activity of TH of acetophenone reaction using complexes **Ru1–Ru4** as a catalyst.

and **Ru3** (Table 3, entries 2 and 4). In comparison to literature reports, the catalytic activities achieved by **Ru1–Ru4** fall within the range of other related Ru(II)–PPh_3 complexes of TOF up to 1.0 × 10^2 h^{-1}.[49–57] However, the catalytic activities of complexes **Ru1–Ru4** are lower compared to some of the highly active ruthenium(II) complexes where the TOFs between 1.0 × 10^4–1.0 × 10^5 h^{-1} were achieved.[58–61]

2.3.4 Investigation of TH reactions using different ketone substrates. We next focused on the investigations of the substrate scope using complexes **Ru4** under the optimised reactions (Table 4). It is significant to note that these complexes formed effective catalysts in the TH of a wide range of ketone substrates, with varied electronic and steric requirements. In general, electron-withdrawing substituents resulted in higher yields compared to those bearing electron-donating groups (Table 4, entries 1–7). For example, using complex **Ru4**, percentage yields of 91%, 97% and 61% were realised for acetophenone,

Table 4 Result of substrate scope studies using complex **Ru4**[a]

Entry	Substrate	Yield[b] (%)	Entry	Substrate	Yield[b] (%)
1	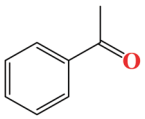	91	9	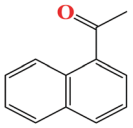	86
2	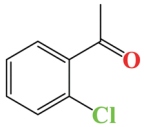	95	10	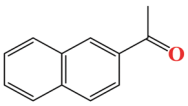	74
3	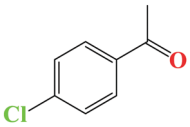	97	11	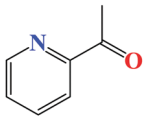	47
4	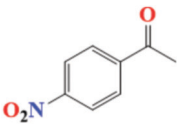	90	12	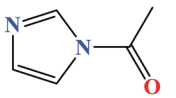	97
5	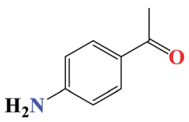	58	13	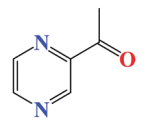	69
6	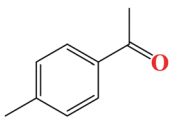	68	14	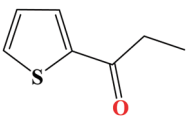	55
8	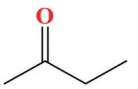	70	15	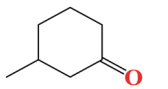	69

[a] General reaction conditions: substrate, 1.00 mmol (1.10 mL): internal standard methoxybenzene, 1.0 mmol (1.12 mL), [**Ru4**], 0.10 mol% (0.93 mg); K^{t}BuO, 2.5 mol% (0.025 mmol) in isopropyl alcohol, temperature 82 °C. reaction time; 6 h. [b] Determined by ^{1}H NMR spectroscopy (all experiments were conducted in triplicate to ensure reproducibility). Methoxy benzene was used as an internal standard.

4-chloroacetophenone and 4-methyl-acetophenone respectively (Table 4, entries 1, 3 and 6). This could be ascribed to the electronic effects of the substituents, where electron-withdrawing groups at the *para* position are known to activate the substrates.[62] Interestingly, no significant effect was observed by changing the position of the substituents. For instance, 4-chloroacetophenone and 2-chloroacetophenone gave yields of 95% and 97% respectively using catalyst **Ru4** (Table 4, entries 2 and 3), pointing to insignificant steric contributions of the chloro substituents.[63,64]

The TH of fused acetophenone substrates as in 1′-acetonaphthone and 2′-acetonaphthone were also accomplished, albeit with lower percentage conversions of 86% and 74% respectively. Notably, complex **Ru4** was capable of reducing even the less reactive heterocyclic substrates (Table 4, entries 11–14). Interestingly, 1′-acetyl imidazole gave high percentage conversions of 97% (Table 4, entry 12). In contrast, the lower yields of, 2′-acetyl pyrazine and 1-(2-thienyl)-1-propanone of 55% (Table 4, entries 13 and 14) could be ascribed to possible irreversible coordination of the nitrogen and sulphur atoms to

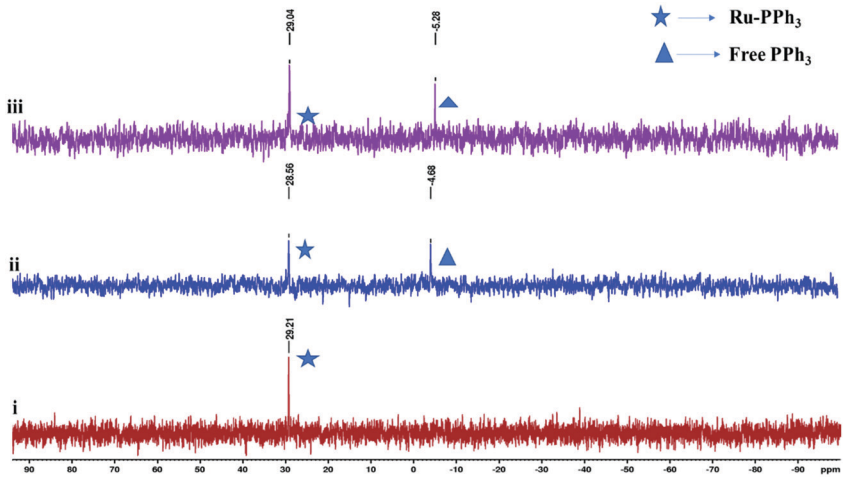

Fig. 3 $^{31}P\{^{1}H\}$ NMR spectral of complex [RuHCO(**L4**)$(PPh_3)_2$], **Ru4** in the presence of acetophenone, ^{i}PrOH and K^{t}BuO for 6 h. Spectrum, (i) shows a signal at δ 23.2 ppm corresponding to two equivalent PPh_3 groups in the complex at t = 0. Spectra (ii) and (iii) show signals for the free PPh_3 at δ −4.7 and 5.28 ppm after 4 h and 6 h respectively.

the active sites of the catalyst.[65,66] The reactivity of the aliphatic ketones was also investigated using 2-propanone (70%) and 3-methyl-2-cyclohexanone (69%) substrates. The lower percentage conversions observed in comparison to acetophenone (91%) under similar reaction conditions (Table 4, entries 1, 8 and 15) could be ascribed to the electron-rich nature of the aliphatic ketones, thus reducing their reactivities.[67]

2.3.5 Proposed mechanism of the transfer hydrogenation of ketones. To gain some insights on the TH reaction mechanism, *in situ* $^{31}P\{^{1}H\}$ NMR spectroscopy experiment was performed in deuterated toluene using catalyst **Ru4** at 60 °C over a period of 6 h (Fig. 3). From the $^{31}P\{^{1}H\}$ NMR spectral data (Fig. 3), a new signal emerged at −5.28 ppm (assigned to the free PPh_3 group) within 1 h, which implicates dissociation of one PPh_3 co-ligand to give the intermediate **Ru4a** (Scheme 2).[10,34] Subsequent coordination of acetophenone substrate to the **Ru4a** species results in the formation of Ru–acetophenone adduct, **Ru4b**. This is followed by the migration of the hydride [Ru–H] from the ruthenium centre to the substrate leading to the generation of intermediate **Ru4c**. Displacement of the protonated substrate from the ruthenium centre by 2-propyl oxide and PPh_3 resulted in the formation of Ru-alkoxide **Ru4d** species as depicted in Scheme 2. This further asserts that the role of the base in this TH mechanism is to assist the regeneration of Ru-alkoxide species.[68] Finally, β-hydride elimination and subsequent release of acetone from the Ru centre lead to regeneration of the active catalyst **Ru4a**.[10,69,70]

3. Conclusions

In this work, we have successfully demonstrated the synthesis, structural studies of carboxamide organo-ruthenium(II/III) complexes bearing PPh_3/CO/Cl/H co-ligands and their applications as catalysts in the TH of ketones. The coordination nature of the Ru(II) complexes was established to consist of one bidentate anionic ligand, and four co-ligands (PPh_3/CO/Cl/H) to give distorted octahedral geometries. All the complexes showed good catalytic activities in the TH of wide range of ketone substrates. More importantly, the Ru–H complexes are capable of promoting the TH reactions under base free conditions. The catalytic activities of the Ru(II) complexes were regulated by the ligand backbone and identity of the auxiliary ligands. In general, Ru–H complexes displayed higher catalytic activities compared to the corresponding Ru–Cl analogues. An inner sphere monohydride mechanism, involving dissociation of one PPh_3 group, was proposed as derived from *in situ* $^{31}P\{^{1}H\}$ NMR spectroscopy studies.

4. Experimental section

4.1 Materials and instrumentation

All the reagents were purchased from Sigma Aldrich and used without further purification. Standard procedures were followed in the purification and drying of solvents.[71] All reactions were performed under an oxygen-free environment unless stated otherwise. The prefabricated ruthenium precursors $[Ru(CO)(PPh_3)_3HCl]$ and $[RuH_2(PPh_3)_3(CO)]$ and were synthesised by adopting a modified procedure.[72–74] The elemental analysis (C, H, N and S) data were recorded on the Thermal Scientific Flash 2000 instrument. The FT-IR spectra of all compounds were recorded on PerkinElmer spectrometer Zn–Se ATR in the range 4000–600 cm^{-1}. All nuclear magnetic resonance, NMR (^{1}H, ^{13}C, ^{31}P) spectra were obtained using a Bruker Avance spectrometer equipped with a Bruker magnet (9.395 T) with chemical shifts relative to tetramethylsilane (^{1}H, ^{13}C) and *ortho*-phosphoric acid (^{31}P). The mass spectra of the compound were recorded on micro-mass LC premier micro-mass spectrometer. The single-crystal X-ray crystallography data were collected on a Bruker Apex II Duo diffractometer coupled with Oxford Instruments.

4.2 X-Ray crystal structure determination

Single crystals suitable for X-ray crystallography analysis were mounted on a glass fibre held with epoxy cement. The single

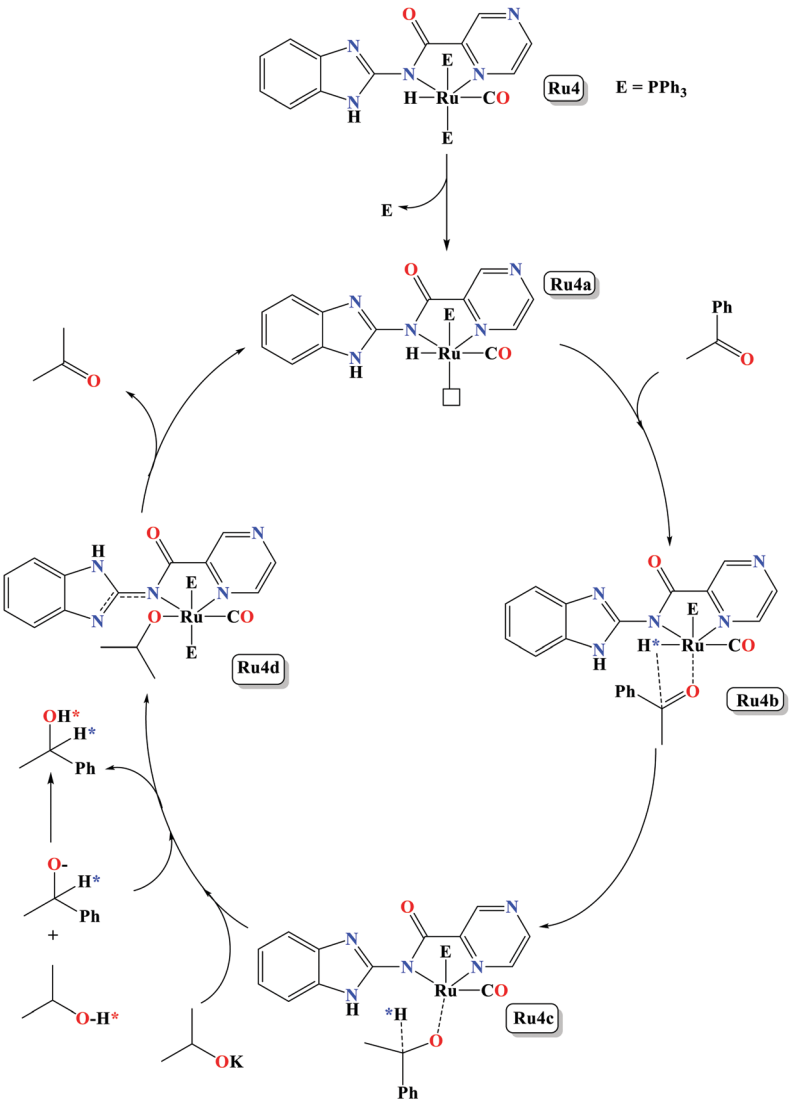

Scheme 2 A proposed monohydride reaction pathway for transfer hydrogenation of ketone catalysed by **Ru4** in the presence of isopropyl alcohol and KOH.

crystals were resized to fit the cross-section diameter of the collimator. The crystallography data of the complexes were collected on Bruker Apex-II CCD at 100 K and graphite monochromated Mo-Kα radiation (λ = 0.71073 Å). The structures were refined using direct methods programmes (SIR-92) and further refined by using a full-matrix least-squares approach on F^2 using SHELXL-2018 and all fundamental calculations were done with the WinGX-2018 crystallographic software.[75] HFIX fixed all hydrogen atoms in ideal places were incorporated in the refinement process using an isotropic thermal model.

4.3 Synthesis and characterization of ruthenium complexes (Ru1–Ru4)

4.3.1 [Ru(L1)(CO)Cl(PPh$_3$)$_2$] (Ru1). A prefabricated [RuHCl-(CO)(PPh$_3$)$_3$] precursor (0.100 g, 0.100 mmol) in ethanol (15 ml) was added to suspension of carboxamide ligand, **HL1** (0.027 g, 0.100 mmol) and the resulting mixture was refluxed at 110 °C to obtain a deep red solution. The crude solution was reduced *in vacuo* to about 3 mL and diethyl ether (25 mL) was added, and the yellow product was collected by filtration and dried *in vacuo*. Single crystals suitable for X-ray analysis were obtained by diffusion of diethyl ether into a saturated solution of the complex in dichloromethane. Yellow solid was obtained. Yield: 0.08 g (85%). ^{1}H NMR (400 MHz, CDCl$_3$) δ_H: 9.15 (d, $^3J_{HH}$ = 4.0 Hz, 1H$_{pyrazine}$), 8.24 (dd, $^3J_{HH}$ = 4.0 Hz, 1H$_{pyrazine}$), 7.88 (d, $^3J_{HH}$ = 3.0 Hz, 1H$_{pyrazine}$), 7.69 (d, $^3J_{HH}$ = 8.0 Hz, 1H$_{benzothiole}$), 7.63 (d, $^3J_{HH}$ = 7.3 Hz, 2H$_{benzothiole}$), 7.45–7.43 (m, 14H), 7.36–7.32 (m, 2H), 7.17 (s, 3H), 7.13–7.15 (m, 2H), 7.04–7.00 (m, 13H). ^{13}C{^{1}H} NMR (101 MHz, CDCl$_3$) δ: 166.9(C-$_{carbonyl}$), 148.2(C-$_{benzothiole}$), 147.8 (C-$_{pyrazine}$), 147.4(C-$_{pyrazine}$), 145.7(C-$_{pyrazine}$), 143.9 (C-$_{pyrazine}$), 134.9(C-$_{benzothiole}$), 133.7(C-$_{benzothiole}$), 131.3 (C-$_{benzothiole}$), 131.1(C-$_{benzothiole}$), 130.7(C-$_{benzothiole}$), 129.6 (C-$_{benzothiole}$), 128.8(C-$_{PPh3}$), 127.8(C-$_{PPh3}$), 124.8(C-$_{PPh3}$), 122.4 (C-$_{PPh3}$), 120.9(C-$_{PPh3}$), 120.6(C-$_{PPh3}$). ^{31}P{^{1}H} NMR (162 MHz,

$CDCl_3$) δ 29.4 (s). FT-IR spectrum (Zn–Se ATR cm^{-1}): 1935 ($\nu C\equiv O)_{Ru-CO}$, 1629 ($\nu C{=}O)_{amidate}$, and 1565 ($\nu C{=}N)_{pyrazine}$. LC-MS: *m*/*z*: calcd 944.08; found 912.15 (M^+–Cl). Anal. calcd for: $C_{49}H_{37}ClN4O_2P_2RuS$: C, 64.51; H, 4.09; N, 6.14; S, 3.40%. Found: C, 64.26; H, 4.01; N, 6.13; S, 3.36%.

Complexes **Ru2–Ru4** were synthesised following the protocol described for **Ru1**.

4.3.2 [Ru(L1)(CO)H(PPh$_3$)$_2$] (Ru2). [$RuH_2(CO)(PPh_3)_3$] (0.100 g, 0.100 mmol) and ligand, **HL1** (0.0280 g, 0.100 mmol). A crystal suitable for X-ray analysis was afforded by diffusion of pentane into a solution of the complexes in dichloromethane. Reddish orange solid compound was obtained. Yield: 0.06 g (65%). ^{1}H NMR (400 MHz, $CDCl_3$): δ_H: −13.26 (t, $^2J_{H-P}$ = 20.3 Hz, $1H_{Ru-H}$), 8.96 (s, $1H_{pyrazine}$), 8.06 (d, $^3J_{HH}$ = 7.9 Hz, $1H_{pyrazine}$), 7.82 (d, $^3J_{HH}$ = 7.8 Hz, $1H_{pyrazine}$), 7.51 (m, 14H), 7.32 (t, $^3J_{HH}$ = 7.5 Hz, 1H), 7.24 (t, $^3J_{HH}$ = 7.4 Hz, 6H), 7.17 (d, $^3J_{HH}$ = 2.9 Hz, $1H_{bz}$), 7.10 (m, 12H). $^{13}C\{^1H\}$ NMR (101 MHz, $CDCl_3$) δ: 166.8($C_{carbonyl}$), 166.3($C_{benzothiole}$), 149.6($C_{pyrazine}$), 149.2($C_{pyrazine}$), 147.9($C_{pyrazine}$), 145.7(C-pyrazine), 134.9-($C_{benzothiole}$), 133.7($C_{benzothiole}$), 132.9($C_{benzothiole}$), 132.7-($C_{benzothiole}$), 132.4($C_{benzothiole}$), 129.7($C_{benzothiole}$), 127.9(C_{PPh3}), 125.0 (C_{PPh3}), 122.2(C_{PPh3}), 121.1(C_{PPh3}), 120.6(C_{PPh3}). $^{31}P\{^1H\}$ NMR (162 MHz, $CDCl_3$) δ 48.2 (s). FT-IR spectrum (Zn–Se ATR, cm^{-1}): 1946 ($\nu C\equiv O)_{Ru-CO}$, 1626 ($\nu C{=}O)_{amidate}$, and 1567 ($\nu C{=}N)_{pyrazine}$. LC-MS, *m*/*z*: calcd 912.12; found 911.08 (M^+–H). Anal. calcd for: $C_{49}H_{38}N_4O_2P_2RuS$: C, 64.68; H, 4.21; N, 6.16; S, 3.52%. Found: C, 64.41; H, 4.30; N, 6.01; S, 3.46%.

4.3.3 [Ru(L2)(CO)Cl(PPh$_3$)$_2$] (Ru3). [$RuClH(CO)(PPh_3)_2$] (0.100 g, 0.110 mmol) and (**HL2**) (0.025 g, 0.110 mmol). Yellow-orange solid. Yield: 0.091 g (88%). ^{1}H NMR (400 MHz, $CDCl_3$): δ 9.08 (s, $1H_{pyz}$), 8.37 (s, $1H_{pyz}$), 8.26 (dd, $^3J_{HH}$ = 4.0 Hz, $1H_{pyrazine}$), 7.56 (t, $^3J_{HH}$ = 3.0 Hz, $1H_{pyrazine}$), 7.52 (s, $2H_{benzothiole}$), 7.29 (d, $^3J_{HH}$ = 8.0 Hz, $2H_{benzothiole}$), 7.25–7.23 (m, 13H), 7.18 – 7.14 (m, 12H). $^{13}C\{^1H\}$ NMR (101 MHz, $CDCl_3$) $^{13}C\{^1H\}$ NMR (101 MHz, $CDCl_3$): δ; 198.1($C_{Ru\equiv CO}$), 168.2-($C_{pyrazine}$), 165.5($C_{benzoimidazole}$), 149.7($C_{pyrazine}$), 148.7($C_{pyrazine}$), 148.4($C_{pyrazine}$), 147.2 ($C_{benzoimidazole}$), 146.9 ($C_{benzoimidazole}$), 133.8($C_{benzoimidazole}$), 126.0(C_{PPh3}), 123.1(C_{PPh3}), 121.8(C_{PPh3}), 120.4(C_{PPh3}). $^{31}P\{^1H\}$ NMR (162 MHz, $CDCl_3$) δ: 42.7 (s). FT-IR spectrum (Zn–Se ATR, cm^{-1}): 1935 ($\nu C\equiv O)_{Ru-CO}$, 1629 ($\nu C{=}O)_{amidate}$, 1562 ($\nu C{=}N)_{pyrazine}$. LC-MS, *m*/*z*: calcd 927.12; found 894.09 [M^+–Cl]. Anal. calcd for: $C_{49}H_{38}ClN_5O_2P_2Ru$: C, 63.47; H, 4.13; N, 7.55. Found: C, 63.96; H, 4.07; N, 6.65.

4.3.4 [Ru(L2)(CO)H(PPh$_3$)$_2$] (Ru4). [$RuH_2(CO)(PPh_3)_3$] (0.100 g, 0.110 mmol) and the corresponding ligand (**HL2**) (0.026 g, 0.110 mmol). Single crystals viable for X-ray analysis were afforded by slow diffusion of diethyl ether into solution of **Ru4** in CH_2Cl_2. Yellow solid compound was obtained. Yield: 0.072 g (75%). ^{1}H NMR (400 MHz, $CDCl_3$) δ_H: −13.12 (t, $^2J_{H-P}$ = 20.1 Hz, $1H_{Ru-H}$), 11.71 (s, 1H), 9.08 (s, $1H_{pyrazine}$), 8.37 (s, $1H_{pyrazine}$), 8.25 (d, $^3J_{HH}$ = 2.9 Hz, $1H_{pyrazine}$), 7.54 (m, 13H), 7.29 (s, 2H), 7.28–7.21 (m, 12H), 7.19–7.13 (m, 7H). $^{13}C\{^1H\}$ NMR (126 MHz, $CDCl_3$) δ: 167.1($C_{carbonyl}$) 155.7($C_{benzimidazole}$), 150.5-($C_{pyrazine}$), 149.5($C_{pyrazine}$), 149.0($C_{pyrazine}$), 147.7($C_{pyrazine}$), 146.9($C_{benzimidazole}$), 145.0($C_{benzimidazole}$), 144.3($C_{benzimidazole}$), 126.8(2$C_{benzimidazole}$), 125.9(2$C_{benzimidazole}$), 124.5(C_{PPh3}), 123.4(C_{PPh3}), 122.4(C_{PPh3}), 121.3(C_{PPh3}). $^{31}P\{^1H\}$ NMR (162 MHz, $CDCl_3$) δ 23.2 (s). FT-IR spectrum (Zn–Se ATR, cm^{-1}): 1946 ($\nu_{C\equiv O})_{Ru-CO}$, 1622 ($\nu_{C=O})_{amidate}$, 1569 ($\nu_{C=N})_{pyrazine}$. LC-MS, *m*/*z*: calcd 893.11; found 892.12 (M^+–H). Anal. calcd for: $C_{49}H_{38}ClN_5O_2P_2Ru$: C, 63.46; H, 4.13; N, 7.55. Found: C, 62.91; H, 6.84; N, 6.37.

4.4 Typical transfer hydrogenation of ketone procedure

A typical procedure was followed, acetophenone (0.12 mL, 1.00 mmol), a solution of KOH (5.4 mg, 0.100 mmol, 10 mol%) in isopropyl alcohol (5 mL) and complex **Ru3** (0.93 mg, 0.001 mmol, 0.1 mol%) to give molar ratio for Ru/KOH/substrate of 1/100/1000 and refluxed at 82 °C for 6 h under nitrogen atmosphere in two necked round-bottomed flask. Anisole (0.11 ml, 1.00 mmol) was introduced in the reaction flask as an internal standard. An aliquot of 0.05 mL of reaction crude was withdrawn using a syringe at regular time intervals, cooled, diluted with dried $CHCl_3$ (0.25 mL), filtered, and the percentage conversions and yields were determined using ^{1}H NMR spectroscopy. The percentage conversions and crude yields were calculated by comparing the integral value of CH_3 of the methoxybenzene (internal standard), substrate (*i.e.* acetophenone) and the 1-phenylethanol product.[76,77] For the mechanistic study, acetophenone (0.11 mL, 1.00 mmol), 0.10 ml of a solution of 2.5 mol% K^{t}BuO in isopropyl alcohol and complex **Ru4** (0.1 mol%) were mixed in (d_8-toluene) and was analyzed using $^{31}P\{^1H\}$ NMR spectroscopy at 65 °C for 6 h.

4.4.1 Isolation of TH products. To isolate the TH product of some selected ketones (*e.g.* acetophenone, 1-acetyl-naphthanone, 2-pentanone and 4-chloroacetophenone, 1.0 mmo1), a solution of K^{t}BuO (5.4 mg, 2.5 mol%), ^{i}PrOH (5.0 mL) and complex **Ru4** (0.93 mg, 0.001 mmol, 0.1 mol%). The crude was cooled to room temperature, and the solvent was evaporated to give a brown crude product. The crude was further purified by column chromatography on silica gel using 5% ethyl acetate/pentanes solution, the eluent was evaporated to obtain the pure product and identified using ^{1}H NMR spectroscopy (Fig. S41–S44, ESI†).

Conflicts of interest

The authors declare no conflict of interest.

Acknowledgements

The authors acknowledge the University of Kwa-Zulu Natal for financial support and Mr Sizwe Zamisa for solving the structures of the complexes.

References

1 J. Louie, C. W. Bielawski and R. H. Grubbs, *J. Am. Chem. Soc.*, 2001, **123**, 11312–11313.
2 D. Wang and D. Astruc, *Chem. Rev.*, 2015, **115**, 6621–6686.

3 J. A. Widegren and R. G. Finke, *J. Mol. Catal. A: Chem.*, 2003, **198**, 317–341.
4 S. Díez-González and S. P. Nolan, *Angew. Chem., Int. Ed.*, 2008, **47**, 8881–8884.
5 D. Astruc, F. Lu and J. R. Aranzaes, *Angew. Chem., Int. Ed.*, 2005, **44**, 7852–7872.
6 H. C. Abbenhuis, *Chem. – Eur. J.*, 2000, **6**, 25–32.
7 V. Dragutan, I. Dragutan, L. Delaude and A. Demonceau, *Coord. Chem. Rev.*, 2007, **251**, 765–794.
8 D. Milstein, *Top. Catal.*, 2010, **53**, 915–923.
9 W.-Y. Chu, C. P. Richers, E. R. Kahle, T. B. Rauchfuss, F. Arrigoni and G. Zampella, *Organometallics*, 2016, **35**, 2782–2792.
10 S. Yadav, P. Vijayan, S. Yadav and R. Gupta, *Dalton Trans.*, 2021, **50**, 3269–3279.
11 S. Yadav, P. Vijayan and R. Gupta, Ruthenium complexes of N/O/S based multidentate ligands: Structural diversities and catalysis perspectives, *J. Organomet. Chem.*, 2021, **954**, 122081.
12 R. Ramachandran, G. Prakash, P. Viswanathamurthi and J. Malecki, *Inorg. Chim. Acta*, 2018, **477**, 122–129.
13 K. Everaere, A. Mortreux and J. F. Carpentier, *Adv. Synth. Catal.*, 2003, **345**, 67–77.
14 A. K. Widaman, N. P. Rath and E. B. Bauer, *New J. Chem.*, 2011, **35**, 2427–2434.
15 D. Huber, P. A. Kumar, P. S. Pregosin, I. S. Mikhel and A. Mezzetti, *Helv. Chim. Acta*, 2006, **89**, 1696–1715.
16 Q.-F. Zhang, F. K. Cheung, W.-Y. Wong, I. D. Williams and W.-H. Leung, *Organometallics*, 2001, **20**, 3777–3781.
17 J. C. Riedel and U. C. Irvine, *PhD thesis, Development and design of transition metal catalyzed transformation of macrocyclization and C–C bond formation*, University of California Irvine, 2019.
18 J. Choi and G. C. Fu, *Science*, 2017, **356**, eaaf7230.
19 K. Ohno, Y. Kataoka and K. Mashima, *Org. Lett.*, 2004, **6**, 4695–4697.
20 P. Yan, C. Nie, G. Li, G. Hou, W. Sun and J. Gao, *Appl. Organomet. Chem.*, 2006, **20**, 338–343.
21 W. Rabten, T. Åkermark, M. D. Kärkäs, H. Chen, J. Sun, P. G. Andersson and B. Åkermark, *Dalton Trans.*, 2016, **45**, 3272–3276.
22 L. He, J. Ni, L. C. Wang, F. J. Yu, Y. Cao, H. Y. He and K. N. Fan, *Chem. – Eur. J.*, 2009, **15**, 11833–11836.
23 Z. Zhang, N. A. Butt, M. Zhou, D. Liu and W. Zhang, *Chin. J. Chem.*, 2018, **36**, 443–454.
24 Y.-Y. Li, S.-L. Yu, W.-Y. Shen and J.-X. Gao, *Acc. Chem. Res.*, 2015, **48**, 2587–2598.
25 R. van Putten, G. A. Filonenko, A. Gonzalez De Castro, C. Liu, M. Weber, C. Müller, L. Lefort and E. Pidko, *Organometallics*, 2019, **38**, 3187–3196.
26 M. Perez, S. Elangovan, A. Spannenberg, K. Junge and M. Beller, *ChemSusChem*, 2017, **10**, 83–86.
27 J. Qin, Z. Zhou, T. Cui, M. Hemming and E. Meggers, *Chem. Sci.*, 2019, **10**, 3202–3207.
28 T. Liu, H. Chai, L. Wang and Z. Yu, *Organometallics*, 2017, **36**, 2914–2921.
29 N. Zotova, F. J. Roberts, G. H. Kelsall, A. S. Jessiman, K. Hellgardt and K. K. M. Hii, *Green Chem.*, 2012, **14**, 226–232.
30 R. M. Alam and J. J. Keating, *Synthesis*, 2021, 4709–4722.
31 P. Melle, Y. Manoharan and M. Albrecht, *Inorg. Chem.*, 2018, **57**, 11761–11774.
32 A. H. Ngo and L. H. Do, *Inorg. Chem. Front.*, 2020, **7**, 583–591.
33 B. Çetinkaya, I. Özdemir, C. Bruneau and P. H. Dixneuf, *Eur. J. Inorg. Chem.*, 2000, 29–32.
34 A. O. Ogweno, S. O. Ojwach and M. P. Akerman, *Dalton Trans.*, 2014, **43**, 1228–1237.
35 R. Reddyrajula and U. Dalimba, *Bioorg. Med. Chem. Lett.*, 2020, **30**, 126846.
36 P. Vijayan, S. Yadav, S. Yadav and R. Gupta, *Inorg. Chim. Acta*, 2020, **502**, 119285.
37 B. P. R. Aradhyula, W. Kaminsky and M. R. Kollipara, *J. Mol. Struct.*, 2017, **1149**, 162–170.
38 P. Vijayan, S. Yadav, S. Yadav and R. Gupta, *Inorg. Chim. Acta*, 2020, **502**, 119285.
39 D. Bansal, G. Kumar, G. Hundal and R. Gupta, *Dalton Trans.*, 2014, **43**, 14865–14875.
40 D. Bansal and R. Gupta, *Dalton Trans.*, 2016, **45**, 502–507.
41 C. R. Groom and I. J. Bruno, *Acta Crystallogr. Sect. B: Structural Sci., Crys. Eng. Mater.*, 2016, **72**, 171–179.
42 I. J. Bruno, J. C. Cole, P. R. Edgington, M. Kessler, C. F. Macrae, P. McCabe, J. Pearson and R. Taylor, *Acta Crystallogr. Sec. B: Struct. Sci.*, 2002, **58**, 389–397.
43 V. Polshettiwar and R. S. Varma, *Green Chem.*, 2009, **11**, 1313–1316.
44 G. K. Ramollo, I. Strydom, M. A. Fernandes, A. Lemmerer, S. O. Ojwach, J. L. Van Wyk and D. I. Bezuidenhout, *Inorg. Chem.*, 2020, **59**, 4810–4815.
45 A. M. Hall, P. Dong, A. Codina, J. P. Lowe and U. Hintermair, *ACS Catal.*, 2019, **9**, 2079–2090.
46 R. Noyori, M. Yamakawa and S. Hashiguchi, *J. Org. Chem.*, 2001, **66**, 7931–7944.
47 K. Abdur-Rashid, A. J. Lough and R. H. Morris, *Organometallics*, 2000, **19**, 2655–2657.
48 S. E. Clapham, A. Hadzovic and R. H. Morris, *Coord. Chem. Rev.*, 2004, **248**, 2201–2237.
49 O. Altan and M. K. Yılmaz, *J. Organomet. Chem.*, 2018, **861**, 252–262.
50 C. S. Cho, B. T. Kim, T.-J. Kim and S. C. Shim, *J. Org. Chem.*, 2001, **66**, 9020–9022.
51 M. Aydemir and A. Baysal, *Polyhedron*, 2010, **29**, 1219–1224.
52 V. Nagalakshmi, R. Nandhini, G. Venkatachalam and K. Balasubramani, *J. Coord. Chem.*, 2020, **73**, 206–216.
53 V. V. Matveevskaya, D. I. Pavlov, T. S. Sukhikh, A. L. Gushchin, A. Y. Ivanov, T. B. Tennikova, V. V. Sharoyko, S. V. Baykov, E. Benassi and A. S. Potapov, *ACS Omega*, 2020, **5**, 11167–11179.
54 N. S. Chowdhury, C. GuhaRoy, R. J. Butcher and S. Bhattacharya, *Inorg. Chim. Acta*, 2013, **406**, 20–26.
55 M. Bala, A. Ratnam, R. Kumar and K. Ghosh, *J. Organomet. Chem.*, 2019, **880**, 91–97.
56 P. Roy, D. Sarkar, P. Ghosh, C. K. Manna, N. Murmu and T. K. Mondal, *J. Mol. Struct.*, 2020, **1204**, 127524.

57 D. A. Cavarzan, C. B. Pinheiro and M. P. de Araujo, *Trans. Met. Chem.*, 2015, **40**, 117–123.
58 W. Baratta, J. Schütz, E. Herdtweck, W. A. Herrmann and P. Rigo, *J. Organomet. Chem.*, 2005, **690**, 5570–5575.
59 T. C. Johnson, W. G. Totty and M. Wills, *Org. Lett.*, 2012, **14**, 5230–5233.
60 W. Baratta, P. Da Ros, A. Del Zotto, A. Sechi, E. Zangrando and P. Rigo, *Angew. Chem., Int. Ed.*, 2004, **43**, 3584–3588.
61 J. Witt, A. Pöthig, F. E. Kühn and W. Baratta, *Organometallics*, 2013, **32**, 4042–4045.
62 A. Maity, A. Sil and S. K. Patra, *Eur. J. Inorg. Chem.*, 2018, 4063–4073.
63 B. Paul, K. Chakrabarti and S. Kundu, *Dalton Trans.*, 2016, **45**, 11162–11171.
64 K. Li, J.-L. Niu, M.-Z. Yang, Z. Li, L.-Y. Wu, X.-Q. Hao and M.-P. Song, *Organometallics*, 2015, **34**, 1170–1176.
65 T. Liu, K. Wu, L. Wang, H. Fan, Y.-G. Zhou and Z. Yu, *Organometallics*, 2019, **39**, 93–104.
66 R. T. Kumah, N. Tsaulwayo, B. A. Xulu and S. O. Ojwach, *Dalton Trans.*, 2019, **48**, 13630–13640.
67 Z. Cao, H. Qiao and F. Zeng, *Organometallics*, 2019, **38**, 797–804.
68 A. M. Kalsin, T. A. Peganova, I. S. Sinopalnikova, I. V. Fedyanin, N. V. Belkova, E. Deydier and R. Poli, *Dalton Trans.*, 2020, **49**, 1473–1484.
69 T. Ohkuma, N. Utsumi, K. Tsutsumi, K. Murata, C. Sandoval and R. Noyori, *J. Am. Chem. Soc.*, 2006, **128**, 8724–8725.
70 J. Wettergren, E. Buitrago, P. Ryberg and H. Adolfsson, *Chem. – Eur. J.*, 2009, **15**, 5709–5718.
71 A. Vogel, *A Text-Book of Practical Organic Chemistry, 846*, ELBS and Longmann, London, 1989.
72 Y. Ogiwara, M. Miyake, T. Kochi and F. Kakiuchi, *Organometallics*, 2017, **36**, 159–164.
73 J. Zhang, H. Wang, Z. Li and C. Wang, *Trans. Met. Chem.*, 1995, **20**, 118–119.
74 M. L. Berch and A. Davidson, *J. Inorg. Nucl. Chem.*, 1973, **35**, 3763–3767.
75 L. J. Farrugia, *J. Appl. Crystallogr.*, 2012, **45**, 849–854.
76 F. Zeng and Z. Yu, *Organometallics*, 2009, **28**, 1855–1862.
77 D. Wang, A. Bruneau-Voisine and J.-B. Sortais, *Catal. Commun.*, 2018, **105**, 31–36.